Available online at www.sciencedirect.com

ScienceDirect

Procedia IUTAM 18 (2015) 96 – 106

Procedia IUTAM

www.elsevier.com/locate/procedia

IUTAM Symposium on Particle Methods in Fluid Mechanics

Unbounded Immersed Interface solver for Vortex Particle-Mesh methods

Y. Marichal[a,*], P. Chatelain[a], G. Winckelmans[a]

[a] *Institute of Mechanics, Materials and Civil Engineering (iMMC)*
Université catholique de Louvain (UCL), B-1348 Louvain-la-Neuve, Belgium.

Abstract

This paper aims at presenting an alternative and more consistent way to account for bodies in the framework of computing incompressible external flows in aerodynamics using vortex particle-mesh methods (VPM). More specifically, we present a purely grid-based numerical technique using an immersed interface method and the James-Lackner algorithm to compute the 2-D potential flow in an unbounded domain, including irregular interior boundaries and also the presence of a given vorticity field. This ingredient is one of the main components that are required for the computation of general viscous flows. It is therefore the first step towards an integrated unbounded immersed interface VPM method.

Selection and/or peer-review under responsibility of the Technical University of Denmark, Department of Mechanical Engineering.

Keywords: Poisson equation; Unbounded domain; Immersed interface method; Boundary integral equation; Potential flow; Vortex method

1. Introduction

Vortex Methods have been studied in the literature for several decades (for an extensive review, see [1] and [2]). They have reached a high level of maturity in terms of theoretical analysis and application. They belong to the class of lagrangian methods, as they handle particles carrying vorticity. This feature is particularly well suited for the computation of incompressible unbounded (or partially bounded) vortical flows (inviscid and viscous) like jets or wakes. In order to improve the computational efficiency, many efforts have been made to combine the particle representation of the flow with an underlying grid, resulting in vortex particle-mesh methods (VPM, see [3] [4]). There, the computation of the spatial differential operators, especially the time consuming solution of the inherent Poisson equation, are performed on the grid.

The integration of solid bodies inside the domain (and the associated no slip condition at the walls) has also been studied thoroughly and different strategies have appeared. Some of them are based on Brinkman-type penalization techniques [5] [6] [7]. Despite their simple formulation and successful application to many different types of flow (bio-locomotion [7], fluid-structure interaction [5], etc.), penalization methods remain problematic, mainly due to the

* Corresponding author. Tel.: +32-10-47-94-60 ; fax: +32-10-45-26-92 .
E-mail address: yves.marichal@uclouvain.be

Selection and/or peer-review under responsibility of the Technical University of Denmark, Department of Mechanical Engineering.
doi:10.1016/j.piutam.2015.11.010

induced smearing of the solution near the body interface and the subsequent local loss of accuracy [8], that is caused by the mollified grid representation of the body force. Another class of techniques is based on Lighthill's wall diffusion model, using a combination of a fast Poisson solver and a boundary element method (here called the *potential flow solver*) to compute, from a given vorticity field, the velocity field that satisfies a no through-flow condition at the wall (using a vortex panel method [9] [10] [11] or a method based on the computation of sources of velocity potential [12]). The residual slip velocity is then diffused into the flow, yielding at convergence the desired no slip condition (some methods directly use the vorticity induced slip velocity for the wall diffusion process [13]). Those methods have shown to perform well for wall-bounded flows (flow past a sphere [14] [11], flow past a moderate aspect ratio wing [11], etc.). However, in the author's opinion, the lack of full consistency between the panel elements and the grid solution may be responsible, in some cases, for time fluctuations of certain diagnostics (such as linear momentum). Therefore, an alternative methodology is sought for and described here, based on the immersed interface method introduced in [15] and further improved in [16] to require only one-dimensional finite difference stencil corrections (*dimension splitting*). Here, the interface is treated in a sharp and consistent way, while keeping the same order of convergence up to the wall. The strategy to enforce a no slip boundary condition at the wall is still based on Lighthill's wall diffusion model; yet, contrary to the vortex panel method, everything is computed on the grid at once.

The aforementioned *potential flow solver* basically solves a Poisson equation in an unbounded domain. For purely lagrangian vortex methods, the boundary condition at infinity is implicitly enforced using Biot-Savart's law through direct or fast summation techniques (FM, fast multipole method in two [17] and three dimensions [18]); yet at a still relatively high computational cost. For VPM methods, one can still use FM for the outer boundary condition needed by the fast finite difference solver [4]. Alternatively, techniques based on fast Fourier transform (FFT) solvers may be used [19] [20], but these remain hardly applicable to immersed interface methods because of the required stencil corrections. We follow here a different approach, based on the James-Lackner algorithm [21] [22], which has been further improved in [23] (and which additionally remains compatible with mesh refinement techniques). In this case however, taking into account interior boundaries involve the need for an iterative approach, as has been shown in [24].

The present work combines the ideas from [16] and [24], and lays the foundations for an alternative numerical technique in the framework of VPM methods to compute consistently the flow past irregularly shaped bodies in an unbounded domain. This paper describes the first step to be performed inside that global methodology, i.e. the computation of the velocity field induced by a given vorticity field with a no through-flow condition at the solid walls, using here a second order finite difference Poisson solver. Section 2 states the problem we are here considering and explains its link with the more general problem consisting in the computation of unsteady viscous flows; Section 3 describes the global algorithm as well as all its necessary ingredients (immersed interface method and James-Lackner algorithm); Section 4 provides some examples and grid convergence study results that confirm the second order accuracy for single and multiple body potential flows with fixed circulation. The problem of how to treat a cusped body such as an airfoil is also handled. The difficulty lies there in the fact that, first the circulation is a priori unknown (as it is prescribed the *Kutta-Joukoswky condition*) and, second, that the solution is moreover singular if the circulation differs from its prescribed value. A way to overcome these problems by enforcing numerically the *Kutta-Joukoswky condition* is proposed. Finally, the grid convergence of this method is assessed.

2. Problem statement

Vortex particle-mesh methods (VPM) are lagrangian methods that solve the Navier-Stokes equations in vorticity-velocity formulation. We here only consider incompressible flows ($\nabla \cdot \mathbf{u} = 0$)

$$\frac{D\boldsymbol{\omega}}{Dt} \triangleq \frac{\partial \boldsymbol{\omega}}{\partial t} + \mathbf{u} \cdot \nabla \boldsymbol{\omega} = (\nabla \mathbf{u}) \cdot \boldsymbol{\omega} + \nu \nabla^2 \boldsymbol{\omega} \qquad \nabla^2 \boldsymbol{\Psi} = -\boldsymbol{\omega} \,,$$

with ν the kinematic viscosity of the fluid. The incompressible velocity field $\mathbf{u}$ can be linked to the vorticity $\boldsymbol{\omega} = \nabla \times \mathbf{u}$ through the above Poisson equation for the streamfunction $\boldsymbol{\Psi}$, as $\mathbf{u} = \nabla \times \boldsymbol{\Psi}$ and $\nabla \cdot \boldsymbol{\Psi} = 0$ (Lorenz' gauge). Numerically, next to the computation of the time evolution of the particles's vorticity (main variable), one additional step therefore consists in solving the Poisson equation, i.e. computing the velocity that is associated to the given vorticity field. For a flow past a non moving body with boundary $\partial\Omega_{int}$, the boundary conditions are $\lim_{|\mathbf{x}|\to\infty} \mathbf{u} = \mathbf{U}_\infty$ (with $\mathbf{U}_\infty$ a constant free stream flow) and $\mathbf{u} = 0$ on $\partial\Omega_{int}$ (no slip condition). The 2-D case ($\boldsymbol{\Psi} = \Psi \mathbf{e}_z$ and $\boldsymbol{\omega} = \omega \mathbf{e}_z$)

is sketched in Fig. 1.

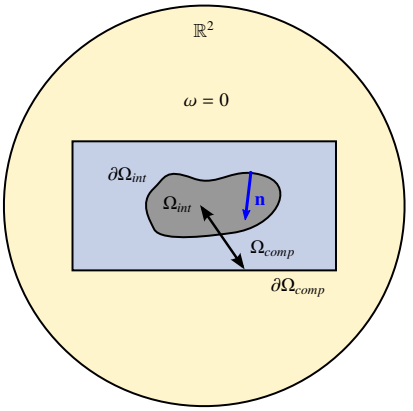

Fig. 1. Sketch of the different domains.

However, the translation of the no slip condition into vorticity formulation is not straightforward. We use here Lighthill's wall diffusion model stating that, at each time step Δt, a vorticity flux can be computed as $\nu\partial\omega/\partial n = \Delta u_s/\Delta t$, where Δu_s is the residual slip velocity resulting from the computation of the velocity field as the solution of the above Poisson equation satisfying a *no through-flow* condition on $\partial\Omega_{int}$ (see [9] [10] for more details). We refer to the latter problem as finding the associated *potential flow* induced by the vorticity field (despite the usual convention that $\omega = 0$), which is the core of the present work.

By abusing the notation slightly, we call $\mathbf{u}$ the potential velocity that satisfies the no through-flow condition $\mathbf{u}\cdot\mathbf{n} = 0$ on $\partial\Omega_{int}$, with $\mathbf{n}$ the inward pointing normal to Ω_{int}. In 2-D, this is equivalent to saying that the streamfunction $\Psi = \overline{\Psi}$ is constant along the boundary $\partial\Omega_{int}$, with $\overline{\Psi}$ a priori unknown. The slip velocity generated by the latter condition can be seen as an infinitely thin vortex sheet (interior boundary charge) $\gamma \triangleq -[\partial\Psi/\partial n]$, with $[a] \triangleq a^+ - a^-$ (a^+ and a^- are respectively the boundary evaluations outside and inside Ω_{int}). Despite the unknown $\overline{\Psi}$, the problem is not under-determined as we also prescribe the circulation $\Gamma \triangleq \oint_{\partial\Omega_{int}} \gamma(\mathbf{x}')\, d\mathbf{x}'$.

Moreover, we assume that the vorticity field is compact and completely included inside the computational domain Ω_{comp} ($\Omega_{int} \subset \Omega_{comp}$), as shown in Fig. 1, and we extend the solution in Ω_{int} with $\Psi = \overline{\Psi}$. By means of the decomposition $\Psi \triangleq \Psi_b + \Psi_\infty$ with $\Psi_\infty = (\mathbf{U}_\infty \times \mathbf{x})\cdot\mathbf{e}_z$ the free stream contribution, we can formally write the set of equations for the unknown body contribution Ψ_b

$$\begin{aligned} \nabla^2\Psi_b &= -\omega \quad \text{in } \Omega_{comp} \\ \Psi_b &= \overline{\Psi} - \Psi_\infty \quad \text{on } \partial\Omega_{int} \quad \text{such that} \quad \oint_{\partial\Omega_{int}} \gamma(\mathbf{x}')\, d\mathbf{x}' = \Gamma \\ \Psi_b &= \Psi - \Psi_\infty \quad \text{on } \partial\Omega_{comp}\,, \end{aligned} \tag{1}$$

with $\overline{\Psi}$ and the outer boundary condition Ψ on $\partial\Omega_{comp}$ being both a priori unknown. Using the free space Green's function for 2-D Poisson equations $G(\mathbf{x}) = \frac{1}{2\pi}\log(|\mathbf{x}|/L)$ (L is a reference length), the solution reads

$$\Psi(\mathbf{x}) = \Psi_\infty(\mathbf{x}) - \int_{\Omega_{comp}} \omega(\mathbf{x}')G(\mathbf{x}-\mathbf{x}')\, d\mathbf{x}' - \oint_{\partial\Omega_{int}} \gamma(\mathbf{x}')G(\mathbf{x}-\mathbf{x}')\, d\mathbf{x}'\,, \tag{2}$$

where γ is part of the solution and thus also a priori unknown.

3. Methodology

This section presents the different components of the the potential flow solver. Section 3.1 details the treatment of the interior boundaries using the immersed interface method; Section 3.2 explains the handling of the outer boundaries using the James-Lackner algorithm; Section 3.3 provides the global algorithm.

3.1. Immersed interface method for the interior boundaries

The method presented here is based on [16] and [25]. Consider a one-dimensional function $f(x) \triangleq f^{(0)}(x) \subset C_\infty(\mathbb{R}\backslash\{x_\alpha\})$ with a discontinuity in x_α (possibly in many derivatives) and some grid points $...,x_{i-1},x_i,x_{i+1},...$ such that $x_\alpha \in [x_i,x_{i+1})$. If the points are equidistant with spacing $h \triangleq x_{i+1}-x_i$ (this constraint can be relaxed, see [16]), one can write for example a jump-corrected finite difference stencil for the second derivative in x_i as

$$\begin{aligned} f^{(2)}(x_i) &= R_{i-1}f^{(0)}(x_{i-1}) + R_i f^{(0)}(x_i) + R_{i+1}\left(f^{(0)}(x_{i+1}) - J_\alpha\right) + \mathscr{O}(h^2) \\ J_\alpha &= [f^{(0)}]_\alpha + \frac{h^+}{1!}[f^{(1)}]_\alpha + \frac{(h^+)^2}{2!}[f^{(2)}]_\alpha + \frac{(h^+)^3}{3!}[f^{(3)}]_\alpha \,, \end{aligned}$$

where $\{R_{i-1},R_i,R_{i+1}\} = \{1,-2,1\}/h^2$ are the coefficients of the uncorrected finite difference stencil, $h^+ \triangleq x_{i+1}-x_\alpha$ and $[f^{(k)}]_\alpha = f^{(k)}(x_\alpha^+) - f^{(k)}(x_\alpha^-)$ is the jump of the k$^{\text{th}}$ derivative $f^{(k)}(x_\alpha)$.

Two- or three-dimensional operators, such as the Laplacian $\nabla^2(\cdot)$, are handled by correcting the derivatives along the different grid directions individually (*dimension splitting* approach). The derivative jumps at the intersections of the interface with the grid lines are computed using one-sided finite difference stencils, the (unknown) boundary condition $\overline{\Psi}$ and the free stream contribution Ψ_∞, depending on which side is in Ω_{int}. The other stencil configurations are treated similarly and are detailed in [16].

Prescribing the circulation is carried out straightforwardly after realizing that the correction terms actually behave like an additional bulk vorticity field [26]. Indeed, if one gathers all the correction terms $J_{\alpha,k}$ that have to be applied at a certain grid point $\mathbf{x}_{ij}$ near the interface, one can write the following equation

$$\left(\nabla^2\Psi\right)_{ij} = -\omega_{ij} - \sum_k \left(-R_k J_{\alpha,k}\right) \triangleq -\omega_{ij} - \left(\omega_\gamma\right)_{ij} \,.$$

ω_γ can be equivalently seen as a discrete projection of the singular vortex sheet γ onto the grid nodes, that is also consistent with the numerical discretization scheme. It is only non-zero in the vicinity of the body interface. The circulation constraint is then, in 2-D :

$$\Gamma = \oint_{\partial\Omega_{int}} \gamma(\mathbf{x}')\, d\mathbf{x}' = \int_{\Omega_{comp}} \omega_\gamma(\mathbf{x}')\, d\mathbf{x}' \simeq \sum_{i,j} \left(\omega_\gamma\right)_{ij} h^2 \,.$$

The resulting system is solved using the library HYPRE [27] [28]; in particular the GMRES solver is combined with an algebraic multigrid preconditioning.

3.2. James-Lackner algorithm for the outer boundary

The methodology adopted here is based on [21] [22] [23], and particularly on [24] for the generalization of the method to problems with an unbounded domain including interior boundaries. Obtaining the outer boundary condition on $\partial\Omega_{comp}$ requires the additional decomposition $\Psi_b \triangleq \Psi_0 + \delta\Psi_b$. The first step of the algorithm consists in computing Ψ_0 as the solution of problem (1), except that $\Psi_0 = 0$ on $\partial\Omega_{comp}$ (and thus also outside of Ω_{comp}). Formally, this results in

$$\begin{aligned} \Psi_0(\mathbf{x}) &= -\int_{\Omega_{comp}} \omega(\mathbf{x}')G(\mathbf{x}-\mathbf{x}')\, d\mathbf{x}' - \oint_{\partial\Omega_{int}} \gamma_0(\mathbf{x}')G(\mathbf{x}-\mathbf{x}')\, d\mathbf{x}' - \oint_{\partial\Omega_{comp}} \gamma_{comp}(\mathbf{x}')G(\mathbf{x}-\mathbf{x}')\, d\mathbf{x}' \\ &= \Psi_b(\mathbf{x}) - \oint_{\partial\Omega_{comp}} \gamma_{comp}(\mathbf{x}')G(\mathbf{x}-\mathbf{x}')\, d\mathbf{x}' + \oint_{\partial\Omega_{int}} (\gamma-\gamma_0)(\mathbf{x}')G(\mathbf{x}-\mathbf{x}')\, d\mathbf{x}' \,, \end{aligned}$$

when comparing with (2). γ_{comp} is an artificial vortex sheet on $\partial\Omega_{comp}$ and has to be cancelled out in $\delta\Psi_b$. The application of Green's third identity gives $\gamma_{comp}(\mathbf{x}) = \nabla\Psi_0(\mathbf{x})\cdot\mathbf{n}$, meaning that this artificial vortex sheet can easily be computed using Ψ_0. Moreover, the body vortex sheet γ_0 that we obtain for Ψ_0 is different from the exact solution γ, because the outer boundary conditions are not yet correct in Ψ_0. This introduces a second correction term in $\delta\Psi_b$ and, using the decomposition, we can write

$$\delta\Psi_b(\mathbf{x}) = \oint_{\partial\Omega_{comp}} \gamma_{comp}(\mathbf{x}')G(\mathbf{x}-\mathbf{x}')\, d\mathbf{x}' - \oint_{\partial\Omega_{int}} (\gamma-\gamma_0)(\mathbf{x}')G(\mathbf{x}-\mathbf{x}')\, d\mathbf{x}' \,.$$

In case there is no body in the domain, no inner vortex sheet are present and the term involving $(\gamma-\gamma_0)$ vanishes in $\delta\Psi_b$. The remaining term involving γ_{comp} is easily accounted for, as we can compute it using Ψ_0. This is the original two-step James-Lackner algorithm [21] [22]. However, as already explained in [24], the presence of the body and the associated vortex sheet on $\partial\Omega_{int}$ makes the task more difficult because $(\gamma-\gamma_0)$ is part of the final solution Ψ_b. At this point, one has to introduce the following iteration :

$$\Psi_b^{(k+1)}(\mathbf{x}) \quad = \quad \Psi_0(\mathbf{x}) + \oint_{\partial\Omega_{comp}} \gamma_{comp}(\mathbf{x}')G(\mathbf{x}-\mathbf{x}')\,d\mathbf{x}' - \oint_{\partial\Omega_{int}} (\gamma-\gamma_0)^{(k)}(\mathbf{x}')G(\mathbf{x}-\mathbf{x}')\,d\mathbf{x}' \,.$$

The way to perform this iteration for Ψ_b and the way to integrate it inside the global methodology is explained in the next Section.

3.3. Global algorithm

The iteration procedure from the previous section is sketched in Fig. 2. Several calls to the immersed interface solver from Section 3.1 are made, after having prescribed a given outer boundary condition on $\partial\Omega_{comp}$. The different steps of the algorithm are

1. Compute the solution Ψ_0 using the immersed interface Poisson solver with homogeneous outer Dirichlet boundary conditions.
2. Obtain the artificial vortex sheet γ_{comp} using one-sided finite differences.
3. Evaluate the contribution of γ_{comp} to Ψ_b on the outer boundary $\partial\Omega_{comp}$, using fast multipole summation techniques with vortex panels. Initialize the iteration index ($k := 0$).
4. Solve for $\Psi_b^{(k+1)}$ using the immersed interface Poisson solver to obtain the solution in Ω_{comp} and increment the iteration index ($k := k+1$).
5. Extract the bulk vorticity field $\left(\omega_{\gamma-\gamma_0}\right)^{(k)}$.
6. Evaluate the new outer boundary condition on $\partial\Omega_{comp}$ due to γ_{comp} and $\left(\omega_{\gamma-\gamma_0}\right)^{(k)}$, using fast multipole summation techniques with singular particles.
7. Assess the convergence by means of the error measure $\|\Psi_b^{(k)} - \Psi_b^{(k-1)}\|_2$ in Ω_{comp}. If it is lower than the prescribed tolerance or the maximum number of iterations has been reached, the procedure stops, else go back to step 4.

4. Results

First, we present the results for the potential flow past a cylinder and with non zero circulation. A convergence study is performed as the analytical solution is known. The present method is also compared to the vortex panel method. The method is then further illustrated and validated in the case of the flow past multiple bodies. Finally, the flow past a cusped airfoil is considered, and we develop an implementation of the *Kutta-Joukowsky condition* that is consistent with the present framework.

4.1. Potential flow past a cylinder

We consider here the potential flow past a circular cylinder of radius R (diameter D) with prescribed circulation, whose solution Ψ_{cyl} can be found in [29]. The circulation is $\Gamma/(4\pi U_\infty R) = 0.5$. The solution is computed on the domain $[-D;D]\times[-D;D]$, using a grid $(N+1)\times(N+1)$, thus defining a mesh size $h \triangleq \Delta x = \Delta y = 2D/N$. As the streamfunction is defined up to a constant, we compute the error field $\varepsilon \triangleq (\Psi-\overline{\Psi}) - \Psi_{cyl}$. We consider the norms $\varepsilon_\infty \triangleq \|\varepsilon\|_\infty \triangleq \max_{\Omega_{comp}}|\varepsilon|$ and $\varepsilon_2 \triangleq \|\varepsilon\|_2 \triangleq (1/D^2\int_{\Omega_{comp}}\varepsilon^2\,d\mathbf{x})^{1/2}$. Results are given in Fig. 3: they confirm an asymptotically second-order behavior in both norms.

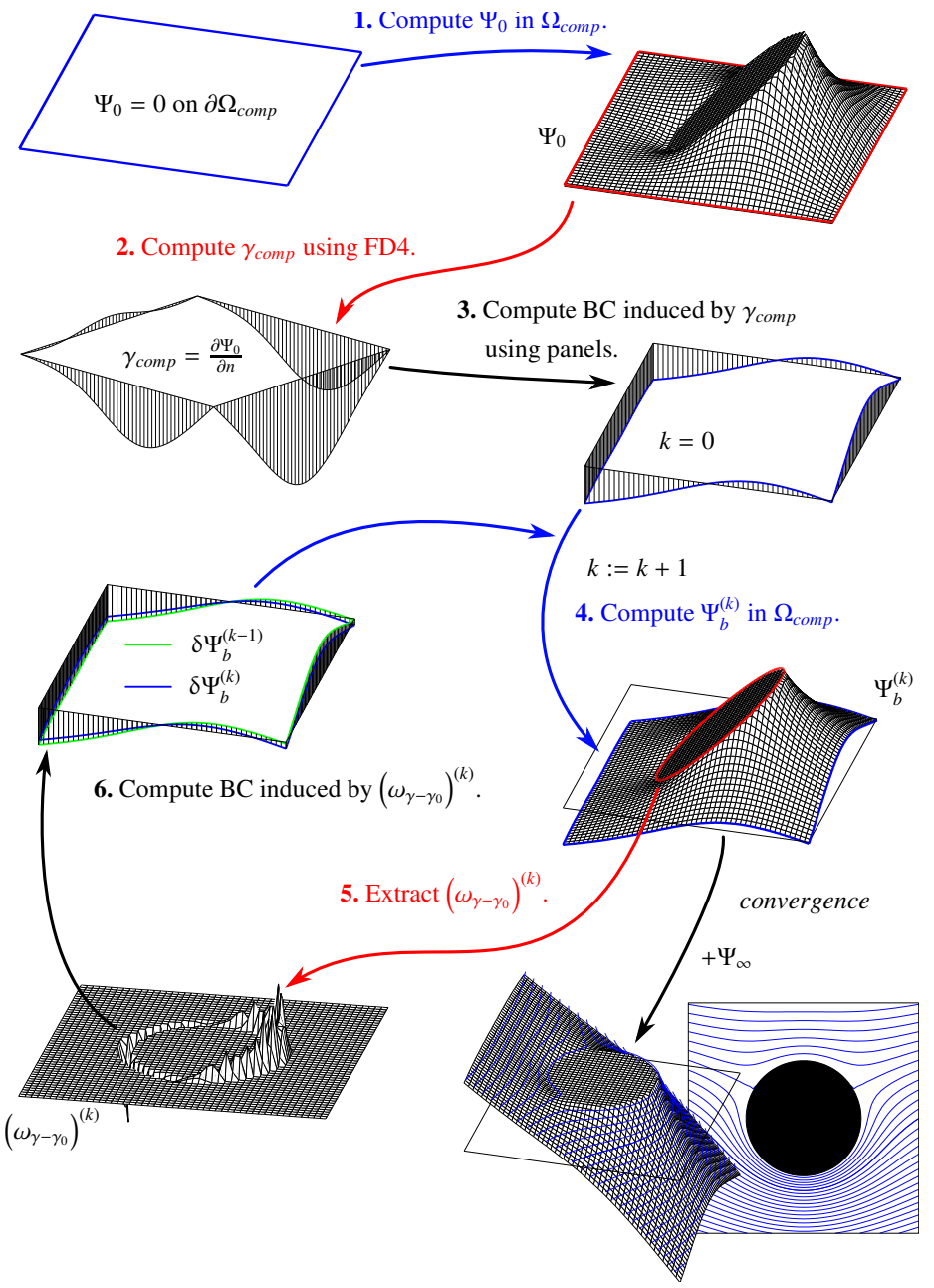

Fig. 2. Sketch of the different computational steps of the algorithm.

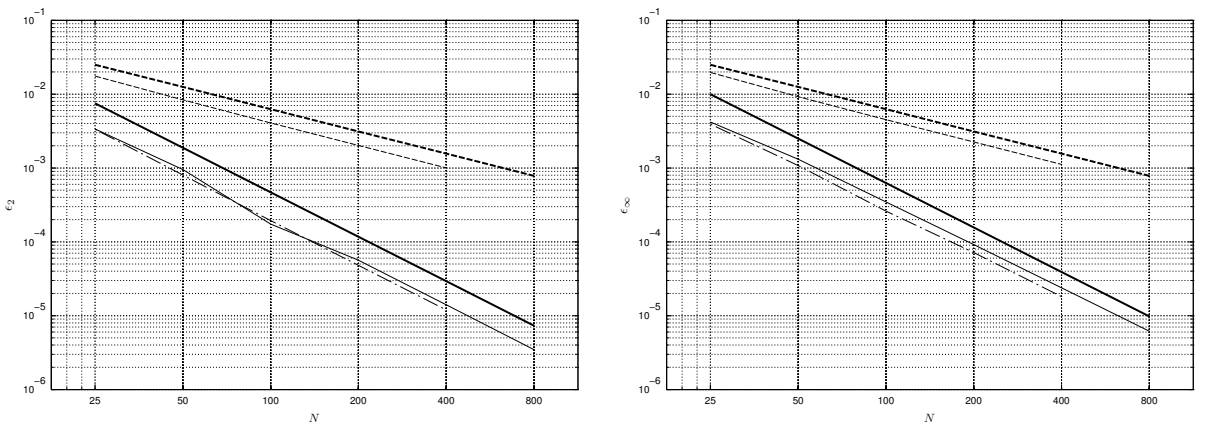

Fig. 3. Grid convergence study for (a) ε_2 and (b) ε_∞ (potential flow past a cylinder): present approach (thin solid), constant panels (thin dashed), linear panels (thin dash-dotted), first-order slope (thick dashed) and second-order slope (thick solid).

In order to allow a comparison with a vortex panel method, we use panels of approximative length h with uniform and linear intensity discretization, and which are respectively first and second-order methods. Grid convergence results for both approaches are also given in Fig. 3. The level of the error for the present approach is found to be similar to that obtained with linear panels. The advantage here is that the representation of the boundary is fully consistent with the underlying finite difference stencil.

4.2. Potential flow past multiple bodies

We now consider the flow with an angle of attack $\alpha = 10^\circ$ past three bodies defined on a domain $[-L;L]\times[-L;L]$, and a grid $(N+1)\times(N+1)$. The bodies are a triangular shape (body 1), a pentagonal shape (body 2) and an ellipse (body 3). Even if some parts of the body geometries are not convex, it is nevertheless guaranteed here that the one-sided correction stencils at the different irregular points do not cross the boundary. The streamlines of the potential flow are given in Fig. 4(a).

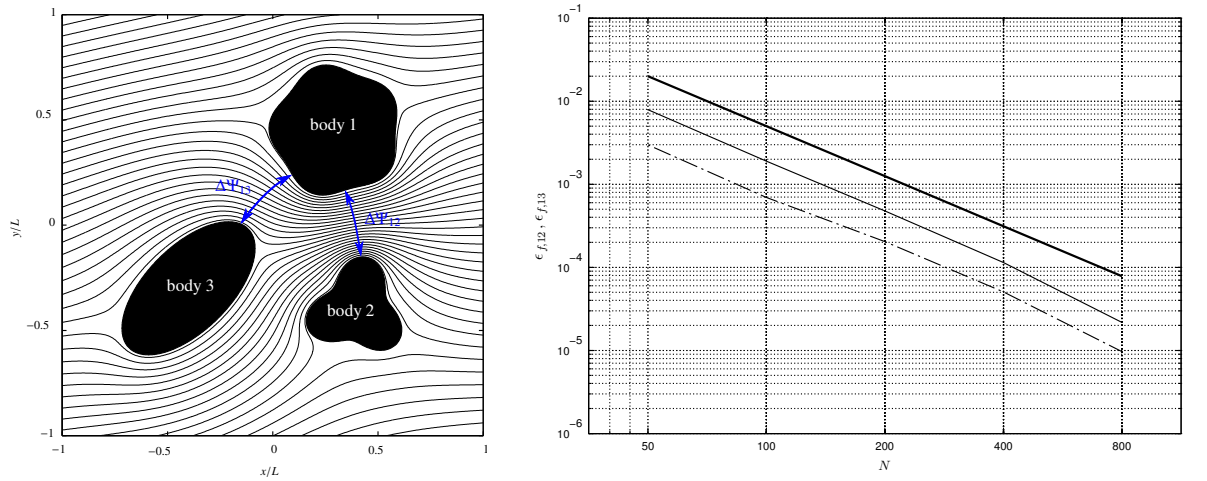

Fig. 4. (a) Computed streamlines for the flow past multiple bodies, using $N = 400$; (b) Grid convergence study for mass flow rates: $\varepsilon_{f,12}$ (thin solid), $\varepsilon_{f,13}$ (thin dashed) and second-order slope (thick solid).

In order to validate the results, the mass flow rates between the bodies are computed: $\Delta\Psi_{12} \triangleq \overline{\Psi}_1 - \overline{\Psi}_2$ and $\Delta\Psi_{13} \triangleq \overline{\Psi}_1 - \overline{\Psi}_3$ ($\overline{\Psi}_m$ is the constant streamfunction value for body m, see also Fig. 4(a)). A mesh convergence study is performed in Fig. 4(b) and one can observe again a second-order convergence for the errors $\varepsilon_{f,12} \triangleq |\Delta\Psi_{12} - \Delta\Psi_{12}^{ref}|$ and $\varepsilon_{f,13} \triangleq |\Delta\Psi_{13} - \Delta\Psi_{13}^{ref}|$, where $\Delta\Psi_{mn}^{ref}$ are the results obtained with the linear vortex panel method.

4.3. Potential flow past an airfoil

The solution Ψ_{jou} for the potential flow past a symmetric Joukowsky airfoil is given in [29]. The angle of attack is here $\alpha = 10°$. The domain is a square defined by $[-L;L] \times [-L;L]$ (with a computational grid $(N+1) \times (N+1)$). The chord is given by $c/L = 1.2$ and the thickness parameter by $\varepsilon/c = 0.035$. The airfoil and the computed streamlines of the flow are displayed in Fig. 5(a).

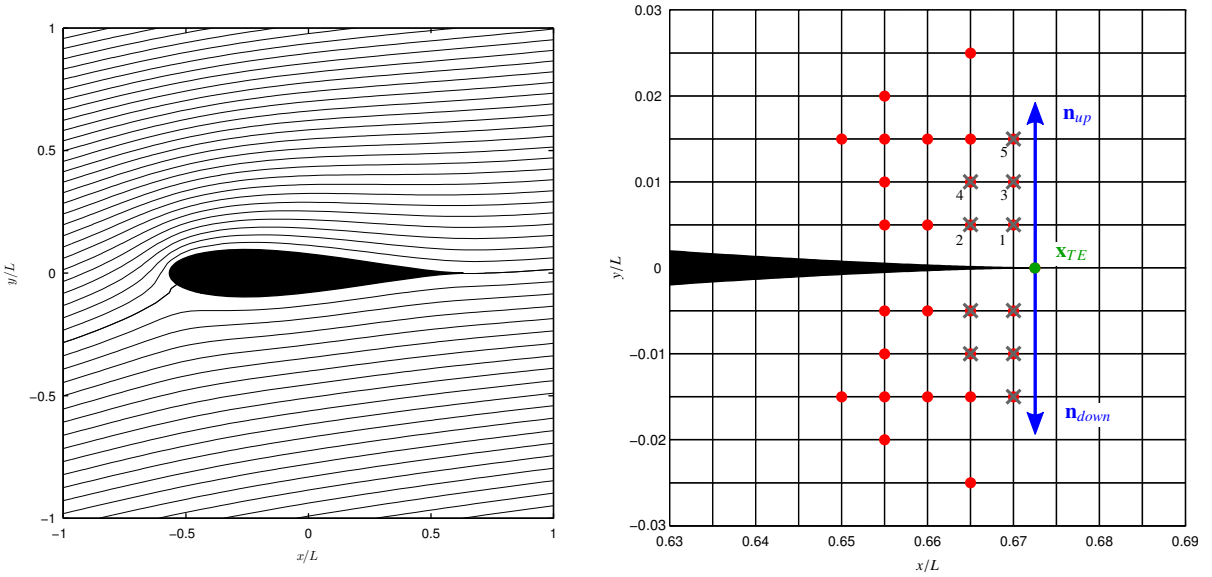

Fig. 5. (a) Computed streamlines for the flow past an airfoil with $\alpha = 10°$, using $N = 50$ and imposing numerically the *Kutta-Joukowsky condition* (with a 2-D stencil of order $p = 1$), the method is seen to perform well despite the low numerical resolution; (b) Stencil used for the discretization of equation (3) (zoom on the trailing edge area). Grid nodes used for $p = 2$ (crosses) and for $p = 4$ (bullets). As an illustration, the weights (for $p = 2$) to compute the derivative $\frac{\partial}{\partial y}(\cdot)$ are $w_{1\ldots5} = \{0, -3, \frac{1}{2}, \frac{9}{2}, -\frac{1}{2}\}/\Delta y$ and $w_{TE} = -\sum_{k=1}^{5} w_k$.

One important feature of the Joukowsky airfoil is the cusped trailing edge. Setting the circulation to $\Gamma_k/(4\pi U_\infty R) = -\sin(\alpha)$ ensures that the velocity vector at the trailing edge remains finite (*Kutta-Joukowsky condition*). The velocity vector is then aligned with the trailing edge (see Fig. 5(a)). Any other choice of Γ leads to an infinite velocity at this point. Yet, for airfoils, the particular required circulation is not known a priori; hence, predicting this circulation is mandatory for potential flow.

Numerically, we have to replace the prescription of the circulation and write a new equation that enforces the proper circulation. As the present approach is iterative, we expect the predicted circulation to change at each iteration step and eventually adopt the correct value, after global convergence. As a consequence, all intermediate solutions have to be assumed singular at the trailing edge. Despite the local singularity, the solution remains regular on both sides of the trailing edge and the proper condition can be equivalently rewritten as :

$$\left.\frac{\partial \Psi_p}{\partial n}\right|_{TE}^{up} + \left.\frac{\partial \Psi_p}{\partial n}\right|_{TE}^{down} = 0\,, \tag{3}$$

where the subscript TE refers to the trailing edge (see Fig. 5(b)). Equation (3) is discretized using two-dimensional finite difference stencils of order p. As an example, two of the resulting stencils for $p = 2$ and $p = 4$ are shown in Fig.

5(b).

The ability of the method to capture this geometric feature, as well as to obtain the correct circulation is tested here in form of a grid convergence study. The trailing edge is placed on a grid line ($y = 0$). Results are shown for ε_∞ in Fig. 6(a) and for $\varepsilon_\Gamma \triangleq |\Gamma - \Gamma_k|$ in Fig. 6(b). The accuracy of the method is here only first order, for both errors, even when increasing the order p of the 2-D stencil. In fact, if the circulation is not equal to Γ_k, the gradient of the solution is infinite in $\mathbf{x}_{TE}$ and so is the jump in the first derivative, which is not taken into account in the present approach. The trailing edge would need a special treatment in order to improve the convergence order. We leave this as a subject for further investigation.

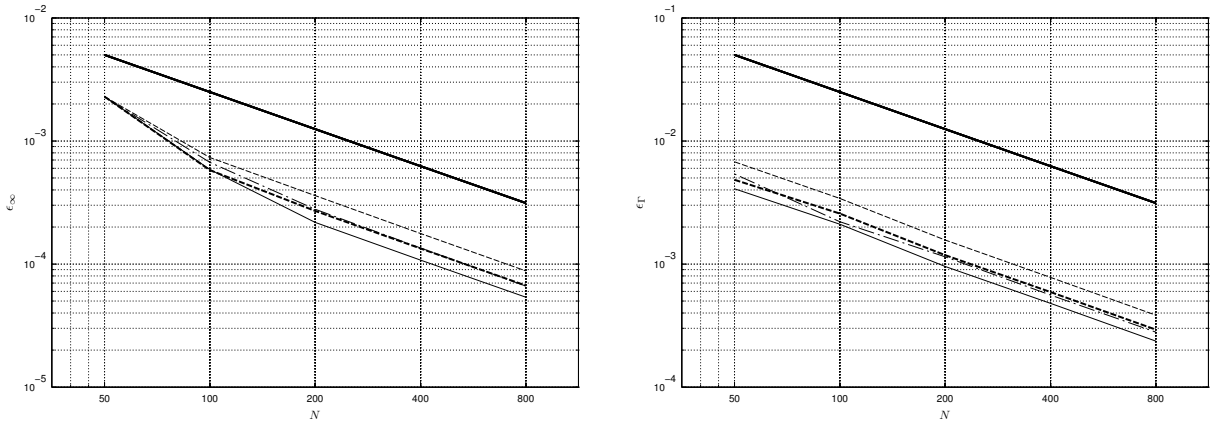

Fig. 6. (Grid convergence study for (a) ε_∞ and (b) ε_Γ (potential flow past an airfoil): $p = 8$ (thin solid), $p = 4$ (thick dashed), $p = 2$ (thin dashed), $p = 1$ (thin dash-dotted) and first-order slope line (thick solid).

5. Conclusion

A two-dimensional second-order finite difference potential flow solver has been presented, based on the immersed interface method for the handling of irregularly shaped bodies and on the James-Lackner algorithm to obtain the solution in an unbounded domain. This type of solver is also required when computing unsteady viscous flows using a vortex particle-mesh (VPM) method combined with Lighthill's wall vorticity diffusion model. In the case of the flow past an airfoil, a way to discretize the *Kutta-Joukowsky condition* has been presented. However, the global method is then only first order accurate.

The integration of this solver inside a VPM method is the next step following this work. It requires some additional ingredients, such as the computation of a grid-consistent wall vorticity flux and its diffusion into the surrounding fluid.

Acknowledgements

Yves Marichal is supported by the Belgian french speaking community F.R.S. - FNRS (Fonds de la Recherche Scientifique) under a PhD fellowship (Aspirant du F.R.S. - FNRS). Many insightful discussions with Matthieu Duponcheel are also acknowledged.

References

[1] Cottet GH, Koumoutsakos PD. In: Vortex Methods: Theory and Practice.. 1st ed. Cambridge University Press; 2000. .

[2] Winckelmans GS. Vortex methods. In: Stein E, de Borst R, Hughes TJR, editors. Encyclopedia of computational mechanics. vol. 3 (Fluids). John Wiley & sons; 2004. .

[3] Christiansen JP. Numerical solution of hydrodynamics by the method of point vortices. J Comp Phys. 1973;13:363–379.

[4] Cocle R, Winckelmans G, Daeninck G. Combining the vortex-in-cell and parallel fast multipole methods for efficient domain decomposition simulations. J Comp Phys. 2008;227:2263–2292.

[5] Coquerelle M, Cottet GH. A vortex level set method for the two-way coupling of an incompressible fluid with colliding rigid bodies. J Comp Phys. 2008;227(21):9121 – 9137.

[6] Rossinelli D, Bergdorf M, Cottet GH, Koumoutsakos P. GPU accelerated simulations of bluff body flows using vortex particle methods. J Comp Phys. 2010;229(9):3316 – 3333.

[7] Gazzola M, Chatelain P, van Rees WM, Koumoutsakos P. Simulations of single and multiple swimmers with non-divergence free deforming geometries. J Comp Phys. 2011;230(19):7093 – 7114.

[8] Tornberg A, Engquist B. Regularization Techniques for Numerical Approximation of PDEs with Singularities. J of Sci Comput. 2002;19:527–552.

[9] Koumoutsakos P, Leonard A, Pépin F. Boundary Conditions for Viscous Vortex Methods. J Comp Phys. 1994;113(1):52 – 61.

[10] Ploumhans P, Winckelmans GS. Vortex methods for high-resolution simulations of viscous flow past bluff bodies of general geometry. J Comp Phys. 2000;165:354–406.

[11] Lonfils T, Winckelmans G. Development of an Immersed Boundary Method using Boundary Elements within a Vortex-In-Cell / Parallel Fast Multipole Method [Proceedings Paper]. Proceedings of the V European Conference on Computational Fluid Dynamics ECCOMAS CFD (Lisbon, Portugal). 2010 June;.

[12] Poncet P. Analysis of an immersed boundary method for three-dimensional flows in vorticity formulation. J Comput Phys. 2009;228:7268–7288.

[13] Cottet GH, Poncet P. Advances in direct numerical simulations of 3D wall-bounded flows by Vortex-in-Cell methods. J Comput Phys. 2004;193(1):136–158.

[14] Ploumhans P, Winckelmans GS, Salmon JK, Leonard A, Warren MS. Vortex methods for direct numerical simulation of three-dimensional bluff body flows: application to the sphere at Re = 300, 500, and 1000. J Comput Phys. 2002;178(2):427–463.

[15] Leveque RJ, Li Z. The Immersed Interface Method for Elliptic Equations with Discontinuous Coefficients and Singular Sources. SIAM J Num Anal. 1994;p. 1019–1044.

[16] Linnick MN, Fasel HF. A high-order immersed interface method for simulating unsteady incompressible flows on irregular domains. J Comp Phys. 2005;204(1):157 – 192.

[17] Greengard L, Rohklin V. A fast algorithm for particle simulations. J Comput Phys. 1987;73:325–348.

[18] Barnes JE, Hut P. A hierarchical O(N log N) force calculations algorithm. Nature. 1986;324:446–449.

[19] Hockney RW, Eastwood JW. Computer Simulation Using Particles. New York: McGraw-Hill; 1981.

[20] Chatelain P, Koumoutsakos P. A Fourier-based elliptic solver for vortical flows with periodic and unbounded directions. J Comp Phys. 2010;229(7):2425 – 2431.

[21] James RA. The solution of Poisson's equation for isolated source distributions. J Comp Phys. 1977;25(2):71 – 93.

[22] Lackner K. Computation of ideal MHD equilibria. Computer Physics Communications. 1976;12(1):33 – 44.

[23] McCorquodale P, Colella P, Balls GT, Baden SB. A Local Corrections Algorithm for Solving Poisson's Equation in Three Dimensions. Communications in Applied Mathematics and Computational Science. 2007;2(1):57–81.

[24] Miller GH. An iterative boundary potential method for the infinite domain Poisson problem with interior Dirichlet boundaries. J Comp Phys. 2008;227(16):7917 – 7928.

[25] Wiegmann A, Bube KP. The Explicit-Jump Immersed Interface Method: Finite Difference Methods For PDE With Piecewise Smooth Solutions. SIAM J Numer Anal. 2000;37:827–862.

[26] Calhoun D. A Cartesian grid method for solving the two-dimensional streamfunction-vorticity equations in irregular regions. J Comput Phys. 2002;176(2):231–275.

[27] Falgout RD, Yang UM. Hypre: a Library of High Performance Preconditioners. In: Preconditioners, Lecture Notes in Computer Science; 2002. p. 632–641.

[28] Falgout RD, Jones JE, Yang UM. Pursuing scalability for hypre's conceptual interfaces. ACM Trans Math Softw. 2005 Sep;31(3):326–350.

[29] Batchelor GK. An Introduction to Fluid Dynamics. Batchelor GK, editor; 2000.